The Canadian Mineralogist
Vol. 55, pp. 867-873 (2017)
DOI: 10.3749/canmin.1700037

DAGENAISITE, A NEW ZINC TELLURATE FROM THE GOLD CHAIN MINE, TINTIC, UTAH, U.S.A.

ANTHONY R. KAMPF[§]

Mineral Sciences Department, Natural History Museum of Los Angeles County, 900 Exposition Boulevard, Los Angeles, California 90007, U.S.A.

ROBERT M. HOUSLEY

Division of Geological and Planetary Sciences, California Institute of Technology, Pasadena, California 91125, U.S.A.

JOE MARTY

5199 East Silver Oak Road, Salt Lake City, Utah 84108, U.S.A.

ABSTRACT

Dagenaisite, $Zn_3Te^{6+}O_6$, is a new mineral from the Gold Chain mine, Tintic district, Juab County, Utah, U.S.A. It is a late-stage secondary phase formed by the oxidative alteration of earlier Te- and Zn-bearing minerals. It is associated with cinnabar, dugganite, eurekadumpite, and gold in vugs in a matrix composed of quartz and dolomite. The mineral occurs as tiny light greenish-gray platelets, generally intermixed with amorphous material, forming porous masses that are apparently replacements of earlier phases. The streak is white, the luster is pearly, and crystals are transparent to translucent. The hardness could not be measured, but appears to be <2 (Mohs). The tenacity is flexible, the fracture is irregular, and cleavage was not observed. The calculated density is 6.00 g/cm^3 for the empirical formula. At room temperature, the mineral is slowly soluble in dilute HCl and rapidly soluble in concentrated HCl. Optical properties could not be determined. Electron-microprobe analyses gave the empirical formula $(Zn_{2.39}Cu_{0.36}Ca_{0.06}Mn_{0.03}As_{0.03}Si_{0.02})_{\Sigma 2.89}Te_{1.02}O_6$. The mineral is monoclinic, space group $C2/c$, with cell parameters a 14.87(2), b 8.88(2), c 10.37(2) Å, β 93.33(2)°, V 1367(4) Å^3, and $Z = 12$. The five strongest lines in the X-ray powder diffraction patterns are [d_{obs} Å(I)(hkl)]: 4.311(30)(310), 3.029(44)(222), 2.744(68)($\bar{3}13, 421$), 2.539(100)($\bar{1}32, \bar{4}22$), and 1.6568(48)($\bar{7}32, 350, \bar{2}44$). The mineral is the natural counterpart of synthetic $Zn_3Te^{6+}O_6$, which has a structure based on an approximate close packing of O atoms in an *hhchhc* sequence along [100].

Keywords: dagenaisite, new mineral, crystal structure, Raman spectroscopy, electron microprobe analysis, Gold Coin mine, Tintic, Utah, U.S.A.

INTRODUCTION

As of June 2017, Mindat lists 174 valid mineral species that have been reported from the Tintic mining district. Eighteen (more than 10%) of these contain essential Te, and six of the seven new minerals previously described from the Tintic district contain essential Te. The type locality for all six of these is the Centennial Eureka mine (*cf*. Pekov *et al*. 2011). Herein we describe the new zinc tellurate dagenaisite, which was discovered at the Gold Coin mine, about 2 km SSE of the Centennial Eureka mine.

The mineral is named dagenaisite (/ ˈdæ gen eɪs aɪt /) for John Dagenais (b. 1945), of Vancouver, British Columbia, Canada. Mr. Dagenais has been an active mineral field collector for nearly 50 years. He has collected and provided for scientific research three new mineral species: joelbruggerite (Mills *et al*. 2009) and auriacusite (Mills *et al*. 2010) from the Black Pine mine (Montana), and chromschieffelinite (Kampf *et al*. 2012) from Otto Mountain (California); he has also provided other potentially new species for study. Since 1998, he has collected at mines in the Tintic district (Utah), amassing a collection of more than 1000 specimens

§ *Corresponding author e-mail address:* akampf@nhm.org

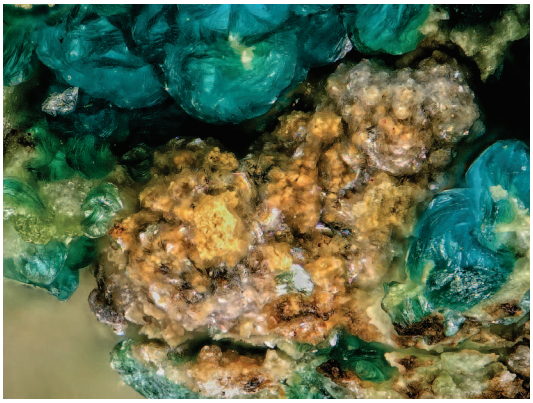

FIG. 1. Hexagonal dagenaisite platelets intermixed with a brownish amorphous phase and associated with blue eurekadumpite rosettes; FOV 0.84 mm across.

encompassing about 120 different species. Mr. Dagenais has given permission for the naming of this mineral in his honor.

The new mineral and name have been approved by the Commission on New Minerals, Nomenclature and Classification of the International Mineralogical Association (IMA2017-017). Four cotype specimens are housed in the collections of the Mineral Sciences Department, Natural History Museum of Los Angeles County, 900 Exposition Boulevard, Los Angeles, California 90007, U.S.A., catalogue numbers 66561, 66562, 66563, and 66564.

Occurrence and Paragenesis

The mineral occurs in the Gold Chain mine, Tintic district, Juab County, Utah, U.S.A. (39°55′44″N 112°6′50″W). The Gold Chain mine exploited a polymetallic (Au-Ag-Cu-Pb-Zn) vein deposit emplaced in dolomite. The upper portion of the deposit is almost completely oxidized (Lindgren & Loughlin 1919).

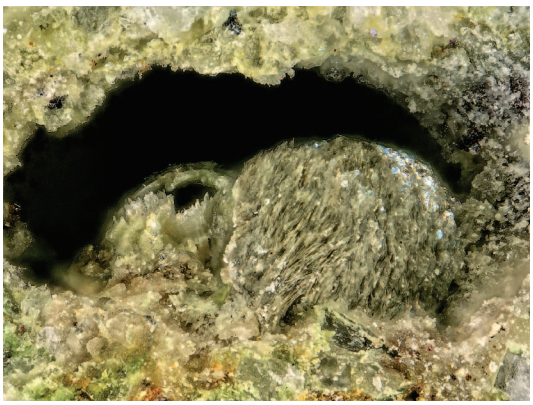

FIG. 2. Dagenaisite plates forming the surfaces of hollow spheres; FOV 1.7 mm across.

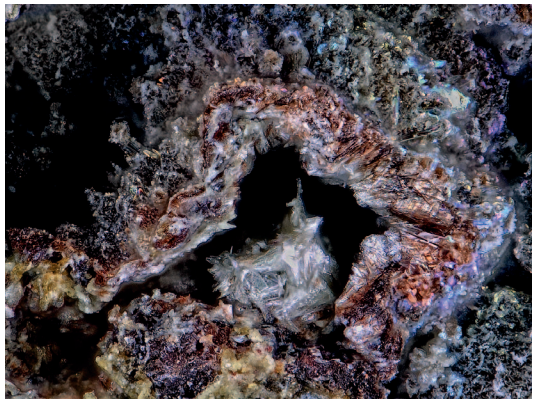

FIG. 3. Dagenaisite plates inside a dagenaisite cast of a crystal (possibly hessite); FOV 0.84 mm across.

Dagenaisite was collected underground from the 300-foot level of the Opohonga stope by one of the authors (JM) on September 22, 2001. The mineral is associated with cinnabar, dugganite, eurekadumpite, and gold in vugs in a matrix composed of quartz and dolomite. Altered remnants, probably of hessite, are embedded in the matrix. Other minerals identified in the general assemblage include adamite, arseniosiderite, atelestite, baryte, beudantite, conichalcite, hemimorphite, kettnerite, malachite, mimetite, mixite, olivenite, and rosasite. Dagenaisite is clearly a late-stage secondary phase formed by the oxidative alteration of earlier Te- and Zn-bearing minerals, probably hessite and sphalerite.

Physical and Optical Properties

Dagenaisite occurs as tiny light greenish-gray plates, generally intermixed with amorphous material, forming porous masses that are apparently replacements of earlier phases. The plates very rarely attain 100 μm in diameter, but are typically much smaller, and are exceedingly thin, usually less than than 1 μm thick (Figs. 1–3). The dagenaisite plates in Figure 1 exhibit hexagonal outlines, which suggests that the plate direction corresponds to {100}, the direction of the hexagonal close-packed layers in the structure. Unfortunately, the extreme thinness of even the largest dagenaisite plates made them unsuitable for single-crystal X-ray diffraction study. Note that SEM examination reveals that dagenaisite crystals in the

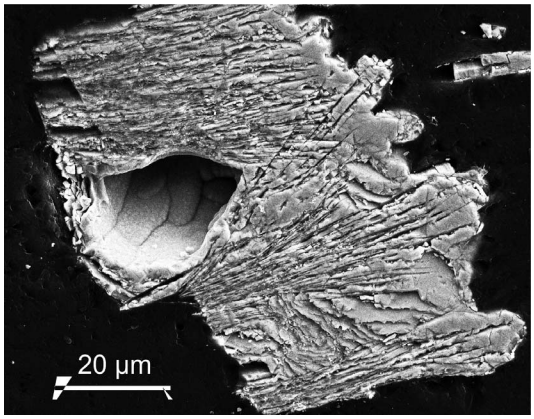

FIG. 4. SEM backscattered image of an intergrowth of dagenaisite and amorphous material. Note that the platy structures do not represent coherent dagenaisite plates, but rather are mixtures of sub-micron dagenaisite crystals and amorphous material.

porous mixtures are often sub-micron in maximum dimension (Fig. 4).

The streak is white, the luster is pearly, and crystals are transparent to translucent. The mineral is non-fluorescent. The hardness could not be measured, but appears to be <2 (Mohs). The tenacity is flexible, the fracture is irregular, and cleavage was not observed. The density could not be measured because it is greater than those of available high-density liquids and there is insufficient material for physical measurement. The calculated density is 6.00 g/cm^3 for the empirical formula. At room temperature, the mineral is slowly soluble in dilute HCl and rapidly soluble in concentrated HCl.

The indices of refraction could not be determined because of the extreme thinness of the plates and their apparent high indices of refraction ($n_{av} = 1.99$ based on the Gladstone-Dale relationship for the empirical formula; Mandarino 1976). Under crossed polars, the crystals exhibit no birefrigence (remain dark) when viewed perpendicular to the plate, but exhibit parallel extinction when viewed on-edge. While the lack of birefrigence when viewed perpendicular to the plate is, in part, due to the thinness of the plates, coupled with the extinction observations noted above, it suggests that the acute bisectrix is approximately normal to the plate direction and that the $2V$ is relatively small. Furthermore, retardation observations from plates oriented on-edge indicate that the crystals are biaxial (+). Assuming, as noted above, that the plate direction is {100}, the optical orientation can be partially given as $Z \approx \mathbf{a}$. No pleochroism was observed.

RAMAN SPECTROSCOPY

Raman spectroscopy was conducted with a Horiba XploRA PLUS instrument. The spectrum recorded between 4000 and 100 cm^{-1} using a 532 nm diode laser exhibited no features indicative of OH or H_2O. Because this spectrum exhibited pronounced fluorescence, a 785 nm diode laser was utilized to record the spectrum from 1600 to 100 cm^{-1}, as shown in Figure 5. Note that the features in the spectrum are poorly resolved, probably reflecting very small coherent domain sizes for phonon scattering in the poorly crystalline material.

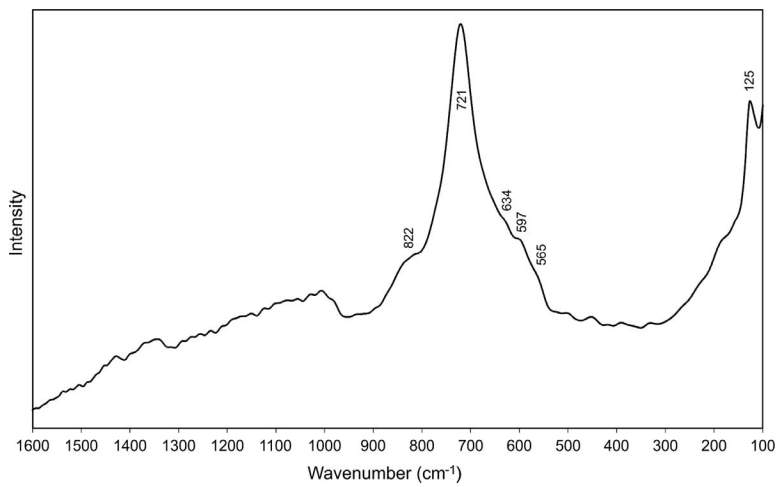

FIG. 5. The Raman spectrum of dagenaisite recorded using a 785 nm laser.

TABLE 1. ANALYTICAL DATA (wt.%) FOR DAGENAISITE

Constituent	Mean	Range	SD	Standard	Normalized
CaO	0.70	0.57–0.84	0.12	syn. anorthite	0.78
CuO	6.22	4.60–7.77	1.35	Cu metal	6.88
MnO	0.42	0.29–0.52	0.10	Mn olivine	0.47
ZnO	42.78	40.11–45.15	0.35	syn. ZnO	47.35
SiO_2	0.23	0.12–0.38	0.10	syn. anorthite	0.25
As_2O_5	0.85	0.25–1.57	0.46	syn. GaAs	0.94
TeO_3	39.15	37.38–41.73	1.89	Te metal	43.33
Total	90.35				100.00

The main band in the spectrum is centered at 721 cm^{-1}, is notably broad, and exhibits indistinct shoulders at approximately 822, 634, 597, and 565 cm^{-1}. Tellurate groups, $Te^{6+}O_6$, have previously been shown to have ν_1, ν_2, and ν_3 bands in this region (*cf.* Blasse & Hordijk 1972, Kampf *et al*. 2013, Frikha *et al*. 2017).

Chemical Composition

Six chemical compositions were obtained with a JEOL8200 electron microprobe (WDS mode, 15 kV, 25 nA, focused beam). Note that the crystal structure known for the synthetic equivalent indicates that the phase is anhydrous and no OH or H_2O was indicated by Raman spectroscopy (which probably also sampled some of the surrounding material). No beam damage was observed. The low totals are attributed to the difficulty in analyzing the very small, thin crystals that form porous aggregates and are intermixed with amorphous phases of similar composition. These intergrowths were impossible to adequately polish and the analyzed volumes always included some pore space and surrounding material. Note that the small amounts of CaO, MnO, SiO_2, and As_2O_5 are probably contained in the surrounding phases and the deviation from stoichiometry in the empirical formula is probably also due to surrounding phases. Both Zn and Te exhibit a negative correlation with Cu, suggesting the possibility that at least some of the Cu in the analyses may be from impurities of a Cu oxide or carbonate. No other elements were detected by EDS. Analytical data are given in Table 1. The empirical formula (based on 6 O *apfu*) is $(Zn_{2.39}Cu_{0.36}Ca_{0.06}Mn_{0.03}As_{0.03}Si_{0.02})_{\Sigma 2.89}Te_{1.02}O_6$. The simplified formula is $(Zn,Cu)_3Te^{6+}O_6$ and the endmember

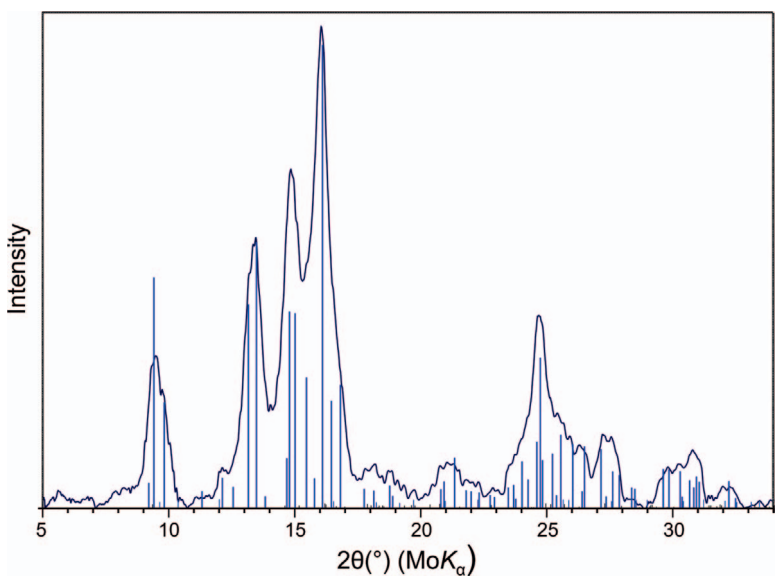

FIG. 6. The powder X-ray diffraction pattern (Mo$K\alpha$) of dagenaisite compared with the lines calculated from the structure of synthetic Zn_3TeO_6.

TABLE 2. POWDER DATA FOR DAGENAISITE COMPARED WITH THE CALCULATED POWDER DATA FOR SYNTHETIC Zn_3TeO_6 (ONLY CALCULATED LINES WITH $I \geq 3$ ARE INCLUDED)

I_{obs}	d_{obs}	d_{calc}	I_{calc}	hkl	I_{obs}	d_{obs}	d_{calc}	I_{calc}	hkl
		4.4171	3	0 2 0			1.6887	3	$\bar{1}$ 3 5
30	4.311	4.3226	36	3 1 0			1.6878	4	7 3 1
13	4.143	4.1423	19	2 0 2			1.6642	16	3 5 0
		3.5954	4	$\bar{2}$ 2 1	48	1.6568	1.6554	35	$\bar{7}$ 3 2
5	3.370	3.3571	6	0 2 2			1.6494	11	$\bar{2}$ 4 4
		3.2433	4	3 1 2			1.6253	8	$\bar{3}$ 1 6
		3.0993	3	$\bar{2}$ 2 2	17	1.6144	1.6240	5	9 1 0
22	3.085	3.0948	39	$\bar{4}$ 0 2			1.6139	3	7 3 2
44	3.029	3.0215	54	2 2 2			1.6043	8	0 2 6
		2.7746	12	1 3 1			1.6032	11	8 2 2
68	2.744	2.7553	47	$\bar{3}$ 1 3	14	1.5870	1.5752	5	3 1 6
		2.7146	46	4 2 1			1.5746	11	7 1 4
16	2.641	2.6357	31	3 1 3			1.5528	4	2 2 6
		2.5829	7	0 0 4	17	1.5524	1.5474	15	$\bar{8}$ 0 4
100	2.539	2.5346	23	$\bar{4}$ 2 2	17	1.5077	1.5107	15	4 4 4
		2.5322	77	$\bar{1}$ 3 2			1.4998	3	$\bar{4}$ 2 6
		2.4803	10	$\bar{2}$ 0 4	17	1.4824	1.4857	9	$\bar{1}$ 3 6
18	2.445	2.4783	14	6 0 0			1.4724	8	0 6 0
		2.4257	14	1 1 4			1.4472	3	1 5 4
		2.4243	12	5 1 2	7	1.4377	1.4409	3	9 3 0
		2.2976	4	$\bar{3}$ 3 2			1.4170	3	$\bar{4}$ 4 5
7	2.251	2.2497	3	3 3 2			1.3873	8	2 6 2
7	2.156	2.1750	4	$\bar{4}$ 0 4	11	1.3884	1.3777	5	$\bar{6}$ 2 6
7	1.9658	1.9647	3	$\bar{5}$ 3 2			1.3770	5	$\overline{10}$ 2 2
		1.9529	4	$\bar{5}$ 1 4			1.3580	4	0 4 6
9	1.9170	1.9151	10	5 3 2	10	1.3611	1.3573	5	8 4 2
		1.8752	3	4 2 4			1.3538	4	0 6 3
7	1.8505	1.8587	5	4 4 1			1.3410	4	7 5 1
		1.8326	4	$\bar{3}$ 3 4	16	1.3322	1.3340	5	$\overline{11}$ 1 1
5	1.7908	1.7951	3	2 2 5			1.3296	8	$\bar{4}$ 6 2
		1.7844	3	3 3 4			1.3249	6	$\bar{5}$ 5 4
9	1.7336	1.7434	5	6 0 4	7	1.2786	1.2778	5	11 1 2
		1.7280	6	1 5 1			1.2676	3	1 1 8
11	1.7013	1.7044	9	$\bar{4}$ 2 5					
		1.7034	4	$\bar{8}$ 2 1					

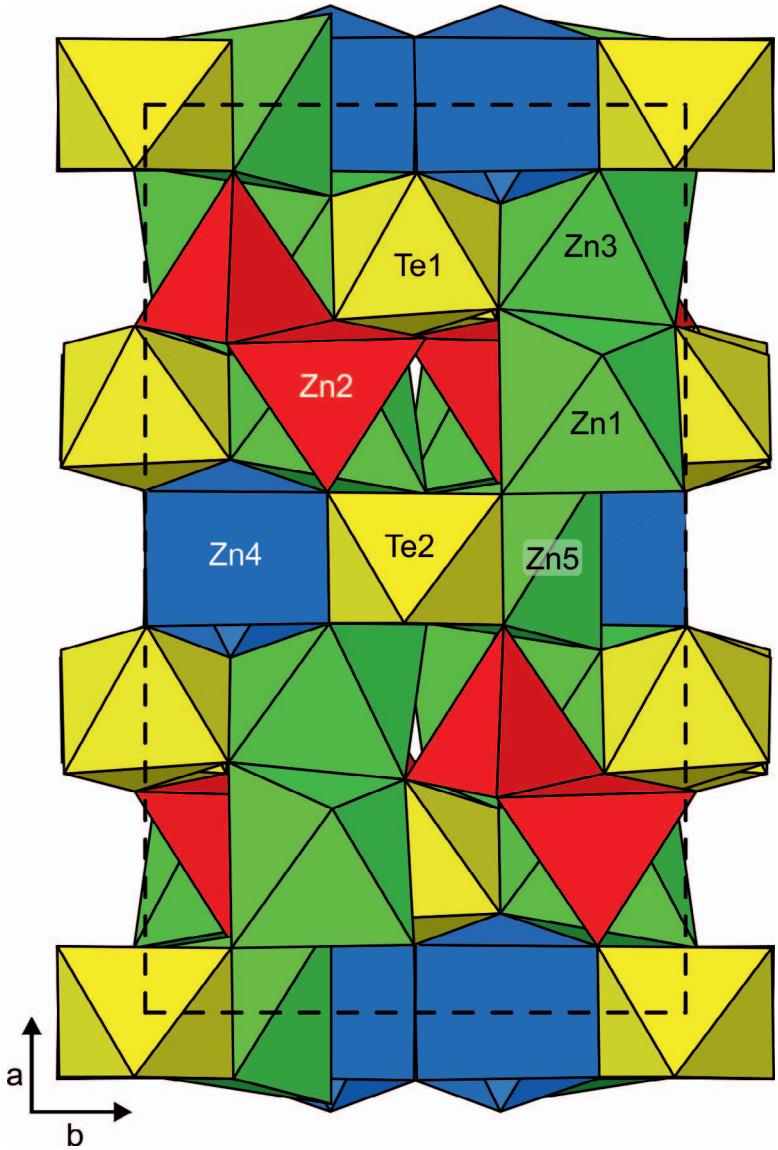

FIG. 7. The crystal structure of synthetic Zn_3TeO_6. The unit-cell outline is shown with dashed lines.

formula is $Zn_3Te^{6+}O_6$, which requires ZnO 58.16, TeO_3 41.84, total 100.00 wt.%.

X-RAY CRYSTALLOGRAPHY

Single-crystal X-ray studies could not be carried out because of the small size and poor quality of the crystals. X-ray powder diffraction data were recorded using a Rigaku R-Axis Rapid II curved imaging plate microdiffractometer with monochromatized Mo$K\alpha$ radiation. Observed d values and intensities were derived by profile fitting using JADE 2010 software (Materials Data Inc.). Data are listed and compared with those calculated from the structure of synthetic Zn_3TeO_6 in Table 2. The close match between the powder diffraction pattern of dagenaisite and the pattern calculated from the structure data for synthetic Zn_3TeO_6 (Weil 2006; Fig. 6) leaves no doubt that dagenaisite has the same structure. Unit-cell parameters refined from the powder data using JADE 2010 with whole-pattern fitting are as follows: monoclinic, $C2/c$, a 14.87(2), b 8.88(2), c 10.37(2) Å, β 93.33(2)°, V 1367(4) Å^3, and $Z = 12$.

Discussion of the Structure

The structure of synthetic Zn_3TeO_6 (Weil 2006; Fig. 7) contains two distinct Te atom positions (Te1 and Te2) with relatively regular octahedral coordinations and five different Zn sites with very different coordinations. The sites Zn1, Zn3, and Zn5 have octahedral coordinations, but Zn1 and Zn3 have quite distorted [4 + 2] coordinations. Zn4 has square pyramidal 5 [4 + 1] coordination and Zn2 has tetrahedral coordination. The substantial amount of Cu^{2+} indicated by the chemical analyses could be accommodated at the Zn1, Zn3, and/or Zn4 sites.

Christy *et al*. (2016) categorized synthetic Zn_3TeO_6 and isostructural Co_3TeO_6 (Becker *et al*. 2006) as structures with neso (monomeric) $Te^{6+}X_6$ groups as part of larger frameworks. They also listed other synthetic phases with structures similar to Zn_3TeO_6, including four with space group $R\bar{3}$ that have a single octahedrally coordinated non-Te cation site (*e.g*., Mg_3TeO_6; Schulz & Bayer 1971) and one with space group $C2$ that has ordered Cu and Zn sites [$Cu_5Zn_4(TeO_6)_3$; Wulff & Müller-Buschbaum 1998]. The latter phase is especially similar structurally to synthetic Zn_3TeO_6. Both of these structures are based on approximate close packing of O atoms in an *hhchhc* sequence along [100] and the two phases have very similar powder X-ray diffraction patterns. By contrast, the $R\bar{3}$ phases have O atom layers (along [001]) that are strongly distorted derivatives of hexagonal close-packing (Schulz & Bayer 1971). Not surprisingly, the powder X-ray diffraction patterns of the $R\bar{3}$ phases are quite different from that of synthetic Zn_3TeO_6 (dagenaisite).

Acknowledgments

Reviewers Stuart Mills and Andrew Christy are thanked for their constructive comments on the manuscript. The microprobe analyses were funded by a grant to Caltech from the Northern California Mineralogical Society. The rest of this study was funded by the John Jago Trelawney Endowment to the Mineral Sciences Department of the Natural History Museum of Los Angeles County.

References

Becker, R., Johnsson, M., & Berger, H. (2006) A new synthetic cobalt tellurate: Co_3TeO_6. *Acta Crystallographica* **C62**, i67–i69.

Blasse, G. & Hordijk, W. (1972) The vibrational spectrum of Ni_3TeO_6 and Mg_3TeO_6. *Journal of Solid State Chemistry* **5**, 395–397.

Christy, A.G., Mills, S.J., & Kampf, A.R. (2016) A review of the structural architecture of tellurium oxycompounds. *Mineralogical Magazine* **80**, 415–545.

Frikha, H., Abdelhedi, M., Mohamed Dammak, M., & Garcia-Granda, S. (2017) Structural single crystal, thermal analysis and vibrational studies of the new rubidium phosphate tellurate $Rb_2HPO_4RbH_2PO_4 \cdot Te(OH)_6$. *Journal of Saudi Chemical Society* **21**, 324–333.

Kampf, A.R., Mills, S.J., Housley, R.M., Rumsey, M.S., & Spratt, J. (2012) Lead-tellurium oxysalts from Otto Mountain near Baker, California: VII. Chromschieffelinite, $Pb_{10}Te_6O_{20}(CrO_4)(H_2O)_5$, the chromate analogue of schieffelinite. *American Mineralogist* **97**, 212–219.

Kampf, A.R., Mills, S.J., Housley, R.M., Rossman, G.R., Marty, J., & Thorne, B. (2013) Lead–tellurium oxysalts from Otto Mountain near Baker, California: XI. Eckhardite, $(Ca,Pb)Cu^{2+}Te^{6+}O_5(H_2O)$, a new mineral with HCP stair-step layers. *American Mineralogist* **97**, 1617–1623.

Lindgren, W. & Loughlin, G.F. (1919) Geology and Ore Deposits of the Tintic Mining District. *United States Geological Survey Professional Paper* **107**, 276 pp.

Mandarino, J.A. (1976) The Gladstone-Dale relationship – Part 1: derivation of new constants. *Canadian Mineralogist* **14**, 498–502.

Mills, S.J., Kolitsch, U., Miyawaki, R., Groat, L.A., & Poirier, G. (2009) Joëlbruggerite, $Pb_3Zn_3(Sb^{5+},Te^{6+})As_2O_{13}(OH,O)$, the Sb^{5+} analogue of dugganite, from the Black Pine mine, Montana. *American Mineralogist* **94**, 1012–1017.

Mills, S.J., Kampf, A.R., Poirier, G., Raudsepp, M., & Steele, I.M. (2010) Auriacusite, $Fe^{3+}Cu^{2+}(As,Sb)O_4O$, a new olivenite-group mineral from the Black Pine mine near Phillipsburg, Montana. *Mineralogy and Petrology* **99**, 113–120.

Pekov I.V., Chukanov N.V., Zadov A.E., Roberts A.C., Jensen, M.C., Zubkova N.V., & Nikischer, A.J. (2011) Eurekadumpite, $(Cu,Zn)_{16}(TeO_3)_2(AsO_4)_3Cl(OH)_{18} \cdot 7H_2O$, a new hypergene mineral. *Geology of Ore Deposits* **53**, 575–582.

Schulz, H. & Bayer, G. (1971) Structure determination of Mg_3TeO_6. *Acta Crystallographica* **B27**, 815–821.

Weil, M. (2006) Zn_3TeO_6. *Acta Crystallographica* **E62**, i246–i247.

Wulff, L. & Müller-Buschbaum, H. (1998) On the Crystal Chemistry of the Copper(II) Zinc Tellurates $Cu_5Zn_4Te_3O_{18}$ and $Cu_{1.5}Zn_{1.5}TeO_6$ with a Note on $Cu_{1.5}Co_{1.5}TeO_6$. *Zeitschrift für Naturforschung* **53b**, 53–57.

Received May 26, 2017. Revised manuscript accepted July 24, 2017.